

PRIVATECHAT: A SECURE ENCRYPTED COMMUNICATION FRAMEWORK WITH BLACK-BOX LLMs

Anonymous authors

Paper under double-blind review

ABSTRACT

With the growing applications of large language models (LLMs), privacy leakage has emerged as a significant concern. However, widely used LLMs are often deployed on cloud platforms and accessible only through relatively expensive API calls, complicating the realization of secure communication between users and cloud LLMs. In this paper, we introduce **PrivateChat**, a novel private communication framework that enables users to safely interact with cloud LLMs using user-customized encryption methods (e.g., *AES*). Our core idea is to learn a private system prompt, which instructs the cloud LLM to process and respond in encrypted text while concealing encryption details from potential attackers. Additionally, to optimize such prompts with few API calls, we propose a Sample-Efficient Simultaneous Perturbation Stochastic Approximation (SE-SPSA) black-box optimization algorithm, which incorporates a baseline-based variance reduction strategy with SPSA for effective and economical training. Extensive experiments on several benchmark datasets with various encryption methods show the effectiveness of our approach in achieving secure and reliable communication with cloud LLMs.

1 INTRODUCTION

In recent years, large language models (LLMs) have been extensively applied in various tasks, such as text generation, language translation, and question answering. However, these LLM applications (e.g., GPT-4 (OpenAI, 2023b) and Claude (Anthropic, 2023)) are often deployed on cloud platforms (i.e., cloud LLMs), posing risks of private information exposure to hackers and service providers in the data transmission process. The privacy risk of LLMs manifests in two main ways: (1) Entity privacy leakage: Users might unintentionally expose their sensitive information (e.g., names, addresses, and age) in their input queries (Lukas et al., 2023); (2) Inference privacy leakage: Potential attackers could deduce personal data (e.g., health, income, and gender) through the user chat records with the LLMs, even if the input text does not explicitly contain private details (Staab et al., 2023). These privacy risks limit the wider applications of LLMs, and many countries have established laws and regulations to restrict and even prohibit their use (Neel & Chang, 2023).

In light of the aforementioned privacy risks associated with using cloud LLMs, secure communication methods are essential. Encryption techniques, such as those employed by communication platforms for ensuring privacy and security, serve as precedents (Lai et al., 2017). This inspires us to explore the feasibility of an encrypted communication framework tailored for interacting with cloud LLMs. This is a novel and highly encouraging research direction, which yet poses a series of new research problems. In detail, to prevent the aforementioned entity and inference privacy leaks to attackers and service providers, both the user query and the LLM’s response should be encrypted during the data transmission process. However, how to enable LLMs to accurately understand and respond to encrypted texts is a non-trivial challenge. In particular, unlike the white-box assumption where the model structure and parameters are accessible, as used in previous privacy-preserving methods (Qu et al., 2021; Zhou et al., 2023), the widely-used emerging LLMs (e.g., GPT-4) are typically black-box, with closed and inaccessible model architectures and parameters. This black-box nature hinders us from directly using the prevalent back-propagation algorithm to fine-tune these black-box LLMs for processing the encrypted texts. Last but not least, even if we could adopt a black-box optimizer, such as SPSA (Spall, 1992a), to fine-tune LLMs through prompt tuning, it would consume numerous sample data for trial-and-error learning (Spall, 2000; 1997a). However,

054
055
056
057
058
059
060
061
062
063
064
065
066
067
068
069
070
071
072
073
074
075
076
077
078
079
080
081
082
083
084
085
086
087
088
089
090
091
092
093
094
095
096
097
098
099
100
101
102
103
104
105
106
107

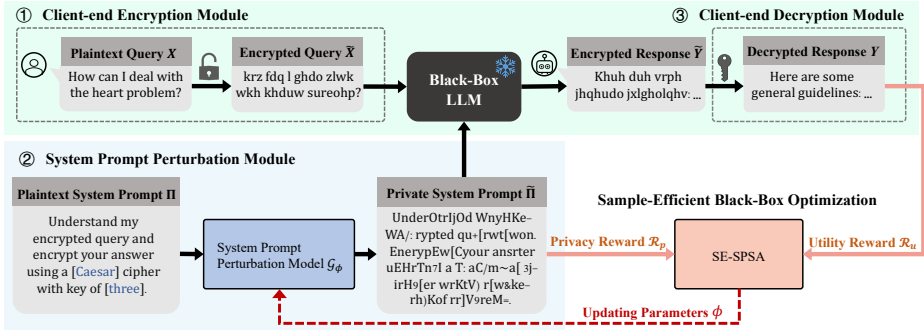


Figure 1: The pipeline of our PrivateChat framework. It enables encrypted communication between users and black-box LLMs under the guidance of a private system prompt. The framework is optimized using our SE-SPSA black-box optimizer, ensuring economical and effective learning.

in our task, training samples are derived from expensive API calls to cloud-based LLMs, making existing black-box optimizers unsuitable.

To address these challenges, we introduce **PrivateChat**, a novel private communication framework ensuring encrypted interactions between clients and cloud black-box LLMs. Our core idea is to train an effective generative model to produce high-quality *private system prompts*, safely written with encryption details, for instructing the cloud LLM to process encrypted queries while safeguarding its encryption details from potential attackers. Specifically, as shown in Fig. 1, our PrivateChat comprises three modules: the client-end encryption module, the system prompt perturbation module, and the client-end decryption module. Our client-end encryption module encrypts the user’s plaintext queries using the user-customized encryption method (e.g., *AES*) and key. Subsequently, our system prompt perturbation module securely embeds these encryption details (i.e., the encryption method and the key) into a system prompt for safely guiding the cloud LLM to process the encrypted query and generate the encrypted response. Next, we submit the encrypted query alongside the private system prompt to the cloud LLM, which returns an encrypted response. Finally, the client-end decryption module decrypts this response into a user-comprehensible plaintext. Note that the generated private prompt can be conveniently reused for subsequent multi-round encrypted dialogues without regeneration. Via such a carefully-designed framework, our PrivateChat enables encrypted communication between users and cloud LLMs, effectively preserving the user privacy.

Nevertheless, it is a non-trivial task to effectively optimize our system prompt perturbation module to produce a desired prompt. First of all, the black-box nature of the cloud LLMs makes the prompt perturbation module non-differentiable, rendering prevalent back-propagation optimization nonfunctional. Moreover, although current black-box optimization methods, such as SPSA (Spall, 1992a), can estimate gradients through trial-and-error learning, such a learning paradigm typically consumes numerous training data samples. In our task, these training samples come from expensive API calls of cloud LLMs, resulting in high training costs. In this paper, these difficulties motivate us to develop a novel black-box optimizer, called Sample-Efficient Simultaneous Perturbation Stochastic Approximation (SE-SPSA), for effective and economical training. Specifically, beyond just using sample data for SPSA-based gradient estimation, we also utilize them to compute an effective baseline for reducing the variance of the gradient estimation. This strategy not only stabilizes and accelerates convergence but also significantly improves the performance by providing more accurate and reliable gradient estimates. Besides, we design two effective reward functions (namely, the utility reward and the privacy reward) as our optimization objectives to ensure both the accuracy of the LLM responses and robust privacy for the private system prompt.

To summarize, our main contributions are as follows: 1) To protect chat content from hackers and service providers, we introduce a novel private communication framework, PrivateChat, enabling safe and encrypted interactions between users and cloud black-box LLMs. To the best of our knowledge, this is the first end-to-end encrypted communication framework between users and cloud black-box LLMs for user privacy protection. 2) We propose a system prompt perturbation module, which generates effective private system prompts for instructing the cloud LLMs to understand and respond to queries with user-customized encryption methods. To tackle the challenges posed by the black-box nature and costly API calls of cloud LLMs during the optimization of our private prompt, we develop a new sample-efficient black-box optimizer, SE-SPSA, which incorporates a baseline-

108 based variance reduction strategy with SPSA for effective and economical training. **3)** Extensive
109 experimental results on different benchmark datasets with various encryption methods including
110 *Caesar*, *DES*, *AES*, and *ChaCha20* demonstrate the outstanding utility and privacy-preserving abil-
111 ities of our framework.

112 113 2 RELATED WORK 114

115 **Large Language Models.** In recent years, numerous large language models (LLMs) like ChatGPT
116 (OpenAI, 2023a;b), LLaMA (AI, 2023), and Claude (Anthropic, 2023), have been developed, show-
117 ing great value in various fields, including code generation (Jain et al., 2023; Gui et al., 2024; Mu
118 et al., 2024), healthcare (Thirunavukarasu et al., 2023; Bazi et al., 2023; Li et al., 2024; Liu et al.,
119 2023a), education (Lee et al., 2024; Bewersdorff et al., 2024), and finance (Ionaşcu, 2023; Muhtar
120 et al., 2024). However, the cloud deployment of commercial LLMs (e.g., GPT-4) raises significant
121 privacy concerns (Yao et al., 2024; Das et al., 2024), as user data transmitted to these services can
122 be vulnerable to interception by hackers or misuse by service providers (Wang et al., 2023). Vari-
123 ous attack methods further highlight the LLMs’ vulnerabilities, such as bypassing LLMs’ security
124 checks to obtain sensitive information (Yuan et al., 2024), and inferring personal privacy through
125 inference attacks (Qu et al., 2021; Dong et al., 2023). While some research efforts (Zhou et al.,
126 2023; Liu et al., 2023b) explore privacy protection in LLM usage, they often require fine-tuning,
127 unsuitable for black-box LLMs with closed architectures. Here, we propose PrivateChat, the first
128 secure encrypted communication framework designed for black-box LLMs, ensuring user privacy.

129 **Privacy-preserving Methods.** Some techniques such as distributed computing (Qin et al., 2014),
130 homomorphic encryption (Ibtihal et al., 2020) and federated learning (Liu et al., 2020) safeguard
131 client data confidentiality, but they require close collaboration between the LLM and the client (e.g.,
132 exchanging model parameters and gradients). This reliance limits their applicability to cloud-based
133 LLMs, which are typically accessible only through commercial APIs. Text sanitization is also a
134 common privacy-preserving method, employing approaches like local differential privacy (Yue et al.,
135 2021; Chen et al., 2023a), which adds random noise during data processing, or anonymization (Chen
136 et al., 2023b; Vats et al., 2023; Kan et al., 2023), which masks or replaces private entities. However,
137 these approaches inevitably incur a certain degree of utility loss (Zhang et al., 2024). Moreover,
138 they only disrupt parts of the user input and fail to protect privacy within LLM responses, allowing
139 attackers to infer private information from both the input context and LLM replies. Here, we are the
140 first to propose a novel framework that enables users to interact with LLMs via ciphertext, ensuring
141 end-to-end privacy protection (e.g., covering both user input and LLM output) without sacrificing
142 information. Furthermore, we design a sample-efficient black-box optimizer to enhance the utility
143 and privacy-preserving capabilities of our framework in a black-box setting.

144 **Black-box optimization.** Traditional black-box optimizers (Lillicrap et al., 2015; Tsai et al., 2020;
145 Spall, 1992a) often use techniques like reinforcement learning (Lillicrap et al., 2015), derivative-free
146 optimization (Ghanbari & Scheinberg, 2017), and one-sided gradient estimators (Tsai et al., 2020)
147 for parameter updates. However, these methods struggle to converge in high-dimensional parameter
148 spaces. Although the simultaneous perturbation stochastic approximation (SPSA) methods (Spall,
149 1992a; Oh et al., 2023) effectively estimates high-dimensional gradients, it usually leads to unstable
150 optimization (Zhao et al., 2011), which, in our task, necessitates numerous expensive API calls
151 to cloud LLMs, resulting in high training times and costs. Moreover, this instability complicates
152 finding optimal solutions, limiting performance. Differently, we propose SE-SPSA, a novel sample-
153 efficient black-box optimizer that combines SPSA with a baseline-based variance reduction strategy,
154 stabilizing gradient estimates and improving optimization reliability and performance with reduced
155 training times and costs.

156 157 3 METHOD

158 In this paper, we propose **PrivateChat**, a novel private communication framework for secure en-
159 crypted interactions between users and cloud LLMs. As shown in Fig. 1, our framework consists
160 of three modules: the client-end encryption module, the system prompt perturbation module, and
161 the client-end decryption module. Given a user’s plaintext query, the client-end encryption module
first encrypts it into ciphertext (Sec. 3.1 (1)). Next, the system prompt perturbation module gen-

erates a private prompt to guide the cloud LLM in processing the ciphertext query and producing an encrypted response without revealing encryption details (Sec. 3.1 (2)). The ciphertext query, along with the private system prompt, is then sent to the cloud LLM. Upon receiving the ciphertext response from the LLM, the client-end decryption module converts it back into plaintext for users to read (Sec. 3.1 (3)). Additionally, we introduce SE-SPSA, a novel sample-efficient black-box optimization framework designed to optimize our framework effectively and efficiently (Sec. 3.2).

3.1 PRIVATE COMMUNICATION FRAMEWORK

(1) Client-end Encryption Module. To prevent chat records from leaking to attackers and service providers, we encrypt user queries on the client end before sending them to the cloud LLM. To this end, we design a client-end encryption module that uses an encryption algorithm with a key to convert the user’s plaintext query X into ciphertext \tilde{X} , as shown in Fig. 1. In particular, our framework allows users to customize their preferred encryption algorithm and key, including both classical encryption algorithms such as *Caesar*, and advanced encryption methods such as *DES*, *AES* and *ChaCha20*, demonstrating its generality. Please refer to Apps. for more details on these encryption methods.

(2) System Prompt Perturbation Module. Upon encrypting the user’s query, we send it to the cloud LLM, expecting a ciphertext LLM response using the identical encryption algorithm utilized for client-end encryption. However, it is challenging for the cloud LLM to directly understand such ciphertext query and provide an encrypted response, as it lacks knowledge of the encryption method and key required to process the ciphertext. One possible solution is to additionally submit a plaintext system prompt to explicitly inform the cloud LLM about the user-customized encryption details. However, this is unsafe, as it directly exposes sensitive encryption details, increasing the risk of privacy leakage. Therefore, our focus is to generate a safe private prompt capable of effectively guiding the LLM to process the encrypted query while concealing the encryption details.

In this paper, we design a system prompt perturbation module to generate such private system prompts. Specifically, we first design an initial plaintext system prompt Π that explicitly instructs the cloud LLM to communicate in a user-customized encryption approach. The initial prompt Π contains the encryption method (e.g., *Caesar*) and the user-defined encryption key, defined by the user at the client-end encryption stage (refer to Sec. 3.1 (1)). A template for this prompt is outlined below:

*“Understand my encrypted query and encrypt your answer
using a [encryption method] cipher with key of [number or binary sequence]”.*

Subsequently, we need to convert this plaintext system prompt Π into a private one $\tilde{\Pi}$. The main challenge here lies in ensuring that this private prompt effectively instructs the cloud LLM (i.e., keeping utility) while simultaneously concealing the encryption details (i.e., keeping privacy), thus achieving both utility and privacy. Given the advanced contextual understanding capabilities of the LLMs, which enable them to discern the underlying semantics of heavily perturbed text (Zhao et al., 2024), we propose a learnable system prompt perturbation model $\mathcal{G}_\phi : \Pi \rightarrow \tilde{\Pi}$ to generate such private prompt $\tilde{\Pi}$ by adaptively perturbing the initial plaintext prompt Π . Here, perturbation means replacing the raw elements (e.g., characters, tokens and words) in the plaintext prompt with the codes from a pre-defined codebook.

Based on our experiments (see Tab. 2), which empirically demonstrate that both word-level and token-level perturbations significantly decrease the LLMs’ performance by hindering their understanding of prompt semantics, we design a more robust character-level perturbation method. Moreover, excessive encryption, such as perturbing all characters in a plaintext prompt, also breaks semantic integrity and contextual cues, resulting in a loss of utility (see Fig. 3). To this end, our system prompt perturbation model adaptively determines which characters to perturb and how to perturb them within the plaintext prompt $\Pi = \{\pi_1, \dots, \pi_N\}$ in order to generate a private system prompt $\tilde{\Pi} = \{\tilde{\pi}_1, \dots, \tilde{\pi}_N\}$ that balances utility and privacy. Here, π_n and $\tilde{\pi}_n$ represent the n^{th} character in the plaintext prompt Π and the private prompt $\tilde{\Pi}$, respectively, where $n \in \{1, \dots, N\}$ and N is the prompt length.

Specifically, our model comprises two types of learnable parameters: the perturbation probability distribution P^P and the encoding probability distribution P^E . The perturbation probability distribution $P^P = \{p_n^P\}_{n=1}^N$ determines which characters in the plaintext prompt should be perturbed,

where p_n^P denotes the probability of perturbing the n^{th} character π_n in the plaintext prompt. For each character π_n , encoding probability distribution P_n^E determines how to perturb it, where $p_{n,r}^E$ represents the probability that the character π_n should be perturbed as C_r (C_r denotes the r^{th} code within a codebook containing a total of R codes, $r \in \{1, \dots, R\}$). To avoid the utility loss caused by the excessive encryption as discussed above, we just perturb the character π_n if its perturbation probability p_n^P exceeds a perturbation threshold ε . Via the above strategy, we produce the private prompt $\tilde{\Pi} = \{\tilde{\pi}_1, \dots, \tilde{\pi}_N\}$ as follows:

$$\tilde{\pi}_n = \begin{cases} C_{r^*}, & \text{if } p_n^P > \varepsilon, \\ \pi_n, & \text{otherwise,} \end{cases} \quad (1)$$

where $r^* = \arg \max_r p_{n,r}^E$ denotes the code index with the highest encoding probability in the codebook corresponding to π_n . Each code in the codebook is a random combination of N_c ASCII characters and for simplicity, we here set $N_c = 1$. By calculating parameter gradients through feedback from the cloud LLM, we can optimize the model parameters $\phi = \{P^P, \{P_n^E\}_{n=1}^N\}$ (refer to Sec. 3.2 for detailed optimization process).

(3) Client-end Decryption Module. As shown in Fig. 1, after obtaining the private system prompt $\tilde{\Pi}$ generated by our prompt perturbation module, we submit it along with the ciphertext queries \tilde{X} to the cloud LLM, and then the LLM can generate a ciphertext response \tilde{Y} . Finally, taking the generated ciphertext response \tilde{Y} as input, the client-side decryption module utilizes the corresponding decryption rules, based on the user-customized encryption method (e.g., *AES*) and key, to convert the encrypted response \tilde{Y} back into the plaintext response Y for the user to read.

3.2 SAMPLE-EFFICIENT BLACK-BOX OPTIMIZATION FRAMEWORK

Utilizing the private communication framework described above enables us to establish secure encrypted interaction between users and cloud LLMs. Within this framework, the generation of effective private system prompts is achieved by training our prompt perturbation model with an optimization objective, which ensures both the privacy and utility of the prompts. However, direct optimization of this objective function using the prevalent gradient back-propagation algorithm is impractical due to the inaccessible architectures of the cloud LLMs (e.g., GPT-4). While traditional black-box optimization methods can estimate gradients by extensively exploring the parameter space, they typically require numerous samples. In our scenario, this would lead to expensive API calls to LLMs, thereby making them inappropriate for our task due to their resource-intensive nature. To achieve a user-friendly system for generating optimal prompts with reduced training time and cost, we propose a sample-efficient black-box optimizer, that enables users to create private system prompts efficiently and economically. Next, we elaborate on our optimization objective and the sample-efficient black-box optimizer.

(1) Privacy Reward and Utility Reward-based Optimization Objective. Our training framework aims to learn an effective private system prompt that guides the cloud LLM to produce highly accurate responses (i.e., utility), while also concealing the encryption details (i.e., privacy). We thus design a utility reward function \mathcal{R}_u to assess the accuracy of LLM response, and a privacy reward function \mathcal{R}_p to evaluate the privacy level of the learned system prompt. These two reward functions are combined as the optimization objective to train our system prompt perturbation model \mathcal{G}_ϕ .

Utility reward. The utility reward \mathcal{R}_u aims to assess the accuracy of the ciphertext responses \tilde{Y} from the cloud black-box LLM. The response accuracy is measured by *Rouge-1* (Lin, 2004), denoted as \mathcal{F}_{Rouge_1} , which calculates the similarity between the groundtruth response Y_{gt} and the decrypted response Y from the cloud LLM:

$$\mathcal{R}_u(Y, Y_{gt}) = \mathcal{F}_{Rouge_1}(Y, Y_{gt}). \quad (2)$$

Privacy reward. The privacy reward \mathcal{R}_p evaluates the privacy level of the generated private system prompt. Based on the fact that a larger difference between the private system prompt $\tilde{\Pi}$ and the original plaintext system prompt Π tends to conceal more privacy information (Qu et al., 2021), we adopt this difference to measure the privacy degree. Specifically, we quantify this difference at both semantic and character levels. Following Sentence-BERT (Reimers & Gurevych, 2019), we calculate the semantic-level difference \mathcal{F}_{sem} based on the cosine similarity Cos between the BERT-based

(Devlin et al., 2018) semantic embeddings of these two prompts (i.e., $\mathcal{F}_{sem}(\Pi, \tilde{\Pi}) = \frac{1 - \text{Cos}(\Pi, \tilde{\Pi})}{2}$). Also, we measure the character-level difference \mathcal{F}_{char} based on the overlap rate $\mathcal{F}_{overlap}$ between the characters of the private and plaintext system prompts (i.e., $\mathcal{F}_{char}(\Pi, \tilde{\Pi}) = 1 - \mathcal{F}_{overlap}(\Pi, \tilde{\Pi})$). Since the critical parts of the system prompt we aim to protect are the encryption details (i.e., the encryption method and key), we further calculate both the semantic and character-level differences between the encryption details in the private and plaintext prompts. Thus, the total privacy reward \mathcal{R}_p can be written as:

$$\mathcal{R}_p(\Pi, \tilde{\Pi}) = \mathcal{F}_{sem}(\Pi, \tilde{\Pi}) + \mathcal{F}_{char}(\Pi, \tilde{\Pi}) + \mathcal{F}_{sem}(\Pi_e, \tilde{\Pi}_e) + \mathcal{F}_{char}(\Pi_e, \tilde{\Pi}_e), \quad (3)$$

where $\tilde{\Pi}_e$ and Π_e represent the encryption details portions of the private prompt and the plaintext prompt, respectively.

In summary, the overall objective function $\mathcal{R}(\phi)$, composed of the utility reward and the privacy reward, can be formulated as:

$$\mathcal{R}(\phi) = \mathcal{R}_u(Y, Y_{gt}) + \mathcal{R}_p(\Pi, \tilde{\Pi}). \quad (4)$$

By maximizing this objective function, we can obtain a private system prompt that ensures privacy and utility. Next, we elaborate on how to optimize this objective function using our carefully-designed sample-efficient black-box optimization algorithm.

(2) Sample-efficient Simultaneous Perturbation Stochastic Approximation (SE-SPSA). To optimize the objective function in Eq. 4, we need to compute the gradients for updating parameters in our system prompt perturbation model so that it can generate effective and private system prompts that maximize the utility and privacy rewards. Since the calculation of the utility reward requires feedback from the cloud black-box LLM, the gradients associated with reward need to be propagated back through the LLM. However, this process is infeasible due to the closed architecture of the black-box LLM. Thus we need to develop a black-box optimizer to estimate parameter gradients through trial-and-error learning. Nevertheless, existing black-box optimizers such as Simultaneous Perturbation Stochastic Approximation (SPSA) (Spall, 1992a), typically consume numerous samples, which are derived from expensive API calls to LLMs in our task, thereby leading to high training costs and time. To handle this challenge, we develop a novel Sample-Efficient SPSA (SE-SPSA) method for effective and economical black-box optimization. In the following, we first introduce SPSA (Spall, 1992a) and then elaborate on our new variant, SE-SPSA, which incorporates a baseline-based variance reduction strategy to stabilize and accelerate the optimization process and improve model performance.

Simultaneous Perturbation Stochastic Approximation (SPSA). Due to the black-box nature of the cloud LLMs, it is infeasible to leverage the back-propagation algorithm to directly compute the analytical gradients of parameters ϕ for optimizing our system prompt perturbation model \mathcal{G}_ϕ using stochastic gradient descent. Therefore, we employ SPSA (Spall, 1992a; 1997b), a black-box optimization method, to estimate the parameter gradients for model optimization. SPSA estimates gradients by randomly perturbing the model parameters ϕ and calculating output differences at these perturbed points. Specifically, at each optimization step, SPSA applies random positive and negative perturbations to the model parameters, measures the differences in the objective function values, and then uses the average of these differences for gradient estimation, termed as \hat{g}_i^{spsa} , which can be formulated as:

$$\hat{g}_i^{spsa}(\phi_i) = \frac{1}{J} \sum_{j=1}^J \frac{1}{\mathbf{u}_i^{(j)}} \left(\frac{\mathcal{R}(\phi_i - c_i \mathbf{u}_i^{(j)}) - \mathcal{R}(\phi_i + c_i \mathbf{u}_i^{(j)})}{2c_i} \right), \quad (5)$$

where $i \in \{0, \dots, I - 1\}$ denotes the optimization step (I is the total number of steps); ϕ_i are the parameters of the system prompt perturbation module in the i^{th} step; $\mathcal{R}(\cdot)$ is our objective function in Eq. 4; c_i is the perturbation coefficient. Following (Oh et al., 2023), $\{\mathbf{u}_i^{(j)} = [u_{i,1}^{(j)}, \dots, u_{i,M}^{(j)}]\}_{j=1}^J$ represent a set of randomly sampled perturbation vectors, where J represents the number of samples and M denotes the dimension of these vectors (i.e., the dimension of the flattened model parameters ϕ). Each vector element $u_{i,m}^{(j)}$ follows a segmented uniform distribution (Spall, 2005; 1992b), specifically $u_{i,m}^{(j)} \sim 0.5 \cdot U(0.5, 1) + 0.5 \cdot U(-1, -0.5)$. With the estimated gradient \hat{g}_i^{spsa} , the parameter update in the i^{th} step of SPSA is written as:

$$\phi_{i+1} = \phi_i - a_i \hat{g}_i^{spsa}(\phi_i), \quad (6)$$

where a_i is the learning rate for the i^{th} optimization step and ϕ_0 denotes the initial model parameters.

Baseline-based Variance Reduction. While SPSA can help estimate parameter gradients under the black-box setting, our experiments (see Fig. 5) empirically show that SPSA suffers from limited training stability and slow convergence in model optimization, which is also observed in previous works (Oh et al., 2023; Spall, 2000). This instability stems from the stochastic nature of the *randomly* sampled perturbation vectors \mathbf{u}_i used in each SPSA optimization step, leading to highly noisy and variable estimated SPSA gradients \hat{g}_i^{spsa} . This causes an unstable optimization path, requiring more optimization steps for effective convergence. In our task, more optimization steps correspond to more expensive API calls to the LLM, significantly increasing training time and cost. Moreover, unstable optimization makes it difficult to achieve optimal results, resulting in poor model performance.

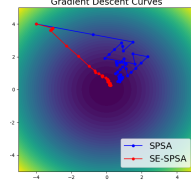


Figure 2: Gradient descent comparison of SPSA and SE-SPSA.

To mitigate this issue, we propose an SPSA-specific variance reduction technique to constrain such stochasticity (i.e., fluctuation amplitude) of the SPSA gradients, enabling faster and more robust convergence. Inspired by baseline-based variance reduction methods (Wu et al., 2018), which theoretically and empirically show that subtracting a suitable constant (termed baseline) can regularize the gradient amplitude to stabilize training, we introduce an SPSA-specific baseline to reduce the variance of SPSA gradients for more stable and accelerated model optimization (See Fig. 2). Formally, we subtract an SPSA-specific baseline value $b_i \in \mathbb{R}$ from the original estimated gradient to form a variance-reduced SPSA gradient estimation $\hat{g}_i^{vr-spsa}$ as follows:

$$\hat{g}_i^{vr-spsa}(\phi_i) = \frac{1}{J} \sum_{j=1}^J \frac{1}{\mathbf{u}_i^{(j)}} \left(\frac{\mathcal{R}(\phi_i - c_i \mathbf{u}_i^{(j)}) - \mathcal{R}(\phi_i + c_i \mathbf{u}_i^{(j)})}{2c_i} - b_i \right). \quad (7)$$

However, it is a non-trivial challenge to obtain the optimal baseline value b_i^* in Eq. 7. To solve this challenge, in our task, we minimize the variance $\text{Var}(\cdot)$ of $\hat{g}_i^{vr-spsa}$ to derive the closed-form solution for the optimal baseline b_i^* through our extensive mathematical analysis, as detailed in Theorem 1.

Theorem 1. *For the baseline-based SPSA gradient estimation in Eq. 7, the optimal baseline b_i^* minimizing the gradient variance has the closed-form solution ($\mathbb{E}[\cdot]$ denotes the expectation):*

$$b_i^* = \frac{\mathbb{E}_{\mathbf{u}_i} \left[\frac{1}{\mathbf{u}_i^\top \mathbf{u}_i} (R(\phi_i - c_i \mathbf{u}_i) - R(\phi_i + c_i \mathbf{u}_i)) \right]}{2c_i \mathbb{E}_{\mathbf{u}_i} \left[\frac{1}{\mathbf{u}_i^\top \mathbf{u}_i} \right]}, \quad (8)$$

where $\mathbf{u}_i = [u_{i,1}, \dots, u_{i,M}]$ and $u_{i,m} \sim 0.5 \cdot U(0.5, 1) + 0.5 \cdot U(-1, -0.5)$.

Proof. We first derive the variance of the baseline-based gradient estimation in Eq. 7:

$$\begin{aligned} \text{Var}(\hat{g}_i^{vr-spsa}) &= \text{Var} \left(\frac{1}{J} \sum_{j=1}^J \frac{1}{\mathbf{u}_i^{(j)}} \left(\frac{\mathcal{R}(\phi_i - c_i \mathbf{u}_i^{(j)}) - \mathcal{R}(\phi_i + c_i \mathbf{u}_i^{(j)})}{2c_i} - b_i \right) \right) \\ &= \frac{1}{J} \left(\frac{1}{4c_i^2} \mathbb{E}_{\mathbf{u}_i} \left[\frac{1}{\mathbf{u}_i^\top \mathbf{u}_i} (R(\phi_i - c_i \mathbf{u}_i) - R(\phi_i + c_i \mathbf{u}_i))^2 \right] + b_i^2 \mathbb{E}_{\mathbf{u}_i} \left[\frac{1}{\mathbf{u}_i^\top \mathbf{u}_i} \right] \right. \\ &\quad \left. - \frac{b_i}{c_i} \mathbb{E}_{\mathbf{u}_i} \left[\frac{1}{\mathbf{u}_i^\top \mathbf{u}_i} (R(\phi_i - c_i \mathbf{u}_i) - R(\phi_i + c_i \mathbf{u}_i)) \right] + b_i^2 \mathbb{E}_{\mathbf{u}_i} \left[\frac{1}{\mathbf{u}_i^\top \mathbf{u}_i} \right]^\top \mathbb{E}_{\mathbf{u}_i} \left[\frac{1}{\mathbf{u}_i^\top \mathbf{u}_i} \right] \right. \\ &\quad \left. + \mathbb{E}_{\mathbf{u}_i} \left[\frac{R(\phi_i - c_i \mathbf{u}_i) - R(\phi_i + c_i \mathbf{u}_i)}{2c_i \mathbf{u}_i} \right]^\top \mathbb{E}_{\mathbf{u}_i} \left[\frac{R(\phi_i - c_i \mathbf{u}_i) - R(\phi_i + c_i \mathbf{u}_i)}{2c_i \mathbf{u}_i} \right] \right. \\ &\quad \left. - 2b \mathbb{E}_{\mathbf{u}_i} \left[\frac{1}{\mathbf{u}_i} \right]^\top \mathbb{E}_{\mathbf{u}_i} \left[\frac{R(\phi_i - c_i \mathbf{u}_i) - R(\phi_i + c_i \mathbf{u}_i)}{2c_i \mathbf{u}_i} \right] \right). \end{aligned} \quad (9)$$

To minimize the variance of $\hat{g}_i^{vr-spsa}$, we set the derivative of the variance with respect to b_i to zero. Given $\mathbb{E}_{\mathbf{u}_i} \left[\frac{1}{\mathbf{u}_i} \right] = 0$ (see Lemma 1 in Apps.), the process is formulated as:

$$\frac{\partial}{\partial b_i} [\text{Var}(\hat{g}_i^{vr-spsa})] = -\frac{1}{Jc_i} \mathbb{E}_{\mathbf{u}_i} \left[\frac{1}{\mathbf{u}_i^\top \mathbf{u}_i} (R(\phi_i - c_i \mathbf{u}_i) - R(\phi_i + c_i \mathbf{u}_i)) \right] + \frac{2}{J} \mathbb{E}_{\mathbf{u}_i} \left[\frac{1}{\mathbf{u}_i^\top \mathbf{u}_i} \right] b_i = 0. \quad (10)$$

□

Table 1: Quantitative comparisons on the SST-2 (Wang et al., 2018), QNLI (Wang et al., 2018) and Medical Q/A (Han et al., 2023) datasets.

Models	SST-2				QNLI				Medical Q/A			
	P_{GS}	$P_{I,LS}$	$P_{O,LS}$	U_{ACC}	P_{GS}	$P_{I,LS}$	$P_{O,LS}$	U_{ACC}	P_{GS}	$P_{I,LS}$	$P_{O,LS}$	$U_{Rouge1/2/L}$
PlainText	0.382	0.000	0.041	0.959	0.257	0.000	0.081	0.919	0.550	0.000	0.628	0.247 / 0.060 / 0.218
SanText(Yue et al., 2021)	0.657	0.836	0.463	0.537	0.668	0.658	0.505	0.495	0.853	0.664	0.817	0.130 / 0.014 / 0.113
SanText+(Yue et al., 2021)	0.566	0.435	0.358	0.642	0.468	0.272	0.503	0.497	0.697	0.347	0.727	0.178 / 0.030 / 0.153
CusText(Chen et al., 2023a)	0.577	0.694	0.390	0.610	0.469	0.262	0.463	0.537	0.720	0.343	0.672	0.200 / 0.038 / 0.178
CusText+(Chen et al., 2023a)	0.571	0.433	0.242	0.758	0.418	0.196	0.372	0.628	0.640	0.116	0.671	0.201 / 0.043 / 0.173
HaS(Chen et al., 2023b)	0.536	0.479	0.137	0.863	0.327	0.142	0.316	0.684	0.563	0.423	0.717	0.177 / 0.025 / 0.151
LeQP	0.769	0.638	0.247	0.753	0.813	0.672	0.486	0.514	0.740	0.513	0.758	0.166 / 0.025 / 0.114
PrivateChat(Caesar)	0.825	0.857	0.999	0.864	0.860	0.800	0.937	0.712	0.864	0.767	0.982	0.232 / 0.045 / 0.211
PrivateChat(DES)	0.837	0.834	0.973	0.856	0.875	0.759	0.949	0.804	0.952	0.714	0.943	0.182 / 0.040 / 0.151
PrivateChat(AES)	0.845	0.889	0.982	0.901	0.835	0.746	0.960	0.813	0.948	0.857	0.974	0.216 / 0.043 / 0.181
PrivateChat(ChaCha20)	0.833	0.842	0.975	0.874	0.907	0.714	0.917	0.796	0.946	0.715	0.972	0.191 / 0.042 / 0.179

Finally, by solving Eq. 10, we derive the optimal baseline b_i^* in Eq. 8 (refer to Apps. for detailed derivations). Given that the expected values in Eq. 8 are intractable due to the continuity of \mathbf{u}_i , we exploit the sample mean to estimate b_i^* as follows:

$$\hat{b}_i^* = \frac{\sum_{j=1}^J \frac{1}{\mathbf{u}_i^{(j)\top} \mathbf{u}_i^{(j)}} \left(R(\phi_i - c_i \mathbf{u}_i^{(j)}) - R(\mathbf{u}_i^{(j)}) \right)}{2c_i \sum_{j=1}^J \frac{1}{\mathbf{u}_i^{(j)\top} \mathbf{u}_i^{(j)}}}. \quad (11)$$

where $\{\mathbf{u}_i^{(j)}\}_{j=1}^J$ are randomly sampled perturbation vectors. Having derived the optimal baseline \hat{b}_i^* via Eq. 11 and substituting it back into Eq. 7, we develop a new variant of SPSA, SE-SPSA, which provides more stable gradient estimation, better approximating the correct gradient direction for more reliable convergence. In our task, this also means fewer API calls to LLMs and more effective prompt generation, thus enabling economical and efficient private conversations with cloud LLMs.

4 EXPERIMENTS

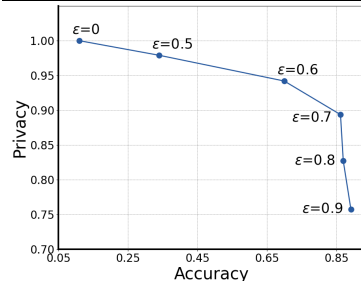
Tasks. Our study focuses on sentiment classification and question-answering (Q/A) tasks. Following (Yue et al., 2021; Chen et al., 2023a), we evaluate our approach on the SST-2 and QNLI classification datasets from the GLUE benchmark (Wang et al., 2018), containing over 1.8k and 5.2k test samples, respectively. To simulate interactions between users and LLMs, we further evaluate our method on the medical Q/A dataset, which contains 100 real-world Q/A pairs from a collaborative medical platform (Han et al., 2023).

Setup. In our system prompt perturbation module, we randomly generate $R = 50$ codes to form a codebook, each code consisting of $N_c = 1$ ASCII character. The perturbation threshold ε is set to 0.7. For the black-box optimization, the optimization steps I is set to 8 and the number of sampled perturbation vectors J is set to 5. Following (Oh et al., 2023), both the perturbation coefficient c_i and the learning rate a_i are dynamically adjustable. Considering the widespread use of GPT-4 (OpenAI, 2023b), we select it as the cloud LLM for training and evaluation. During the training phase, we use 5 samples from the SST-2 training dataset (Wang et al., 2018) for prompt optimization.

Comparison Methods. We compare our PrivateChat with two main types of privacy-preserving methods: (i) **Local Differential privacy (LDP) methods** (*SanText* (Yue et al., 2021) and *CusText* (Chen et al., 2023a)), which enhance privacy by adding noise to input data. (ii) **Anonymization method** (i.e., *HaS* (Chen et al., 2023b)), which employs a local LLM to replace privacy entities (e.g., names, numbers, and locations) with synonyms. Notably, LDP requires model fine-tuning to maintain utility, while anonymization methods focus solely on masking private entities. As a result, neither approach is well-suited for comprehensive protection in our daily chat scenarios. However, since these methods are not dependent on specific LLM architectures, they can be adapted to our

Table 2: Results on different private system prompts.

Models	P_{GS}	$P_{I,LS}$	$P_{O,LS}$	U_{ACC}
DP-based Prompt	0.756	0.654	0.540	0.455
Anon-based Prompt	0.736	0.250	0.860	0.596
Token-level	0.667	0.571	0.950	0.769
Word-level	0.794	0.714	0.802	0.657
Character-level (Ours)	0.825	0.857	0.999	0.864

Figure 3: Privacy & utility performance with different perturbation threshold ε .

432 **Private System Prompt:**
 433 Wo wilkwoe[atvsn'er edcWypnio0]Tian'a9d to exmunicatqh. I wroleivde4[e ke@. Init'arvct'r , and enPry19d que%y encoded%imvbae: ser_D@fole.
 Corresponding plaintext: "We will use the advanced encryption standard to communicate. I will provide the key, initial vector, and encrypted message encoded in base sixty-four."
 434 **Encrypted User Query:**
 435 7UYaNYaddPXmmZhybuCluQ==JhebvgrRRedpw7Ej6kH0dKA==NHN81KmsEbar89jNWz/H9C8+XKzO66DBGaez2M55KNWX1388vBVkZ6ml2pey1WLYHpkasOtvuEX+Y+6ZoxGdiR4Q3bPlDbJfFeessuaqlvF9pBa+u8X
 aP0AjsyUrf0w84M6aFv+TOCKNPLos6adhEX98dBR3S0i+9Hqbl+
 Corresponding plaintext: "b'xcedf'x1a5x86x9dix5x6x99x98on'xe0'x88'xb9' b'4c'x17x9b'x8e'x04Qy'xdap'x9c'f'x'fa'x90'ix1d Answer the question: What to expect if I have Porphyria (Outlook/Prognosis)? Answer:
 436 **GPT-4 Response:**
 437 08JCDe0Pkiw6e2K9DdegecEstxPEVjbfFF94qantHjQ'xGjsVksYHgl1ZTSQkTBJWzUNjakDfDtl72Eyy+Yfel+O7ZM0L VzX6bS10hFyqQifu+zxPsohYIRYoyHUbjPpkrLHH0Cx+gH+XRyeyfSdnSbqvelHJpMLYVvyVSS14
 gYwFCpNFuimV+hQhW9by0eZO9jH6qBP7APWxiMdfS7XcNzrhQIMJoxG2WU/V TqfwPCEAFpV9r1F78P9FQQQAzaiG+sn8jxvgu82g==
 Corresponding plaintext: porphyria varies widely depending on the specific type and severity. Some forms are manageable with treatment and lifestyle adjustments, while others may cause more severe health issues.

Figure 4: An encrypted medical Q/A example with GPT-4 (OpenAI, 2023b) under PrivateChat.

441 setting. Additionally, we design another baseline for comparison: (iii) **Learnable query pertur-**
 442 **bation (LeQP)**, that maps plaintext user queries into perturbed text with a learnable perturbation
 443 model. The model is trained with our SE-SPSA optimizer, using 200 samples from the SST-2 train-
 444 ing dataset (Wang et al., 2018). Unlike our PrivateChat, which employs encryption algorithms to
 445 protect user queries while perturbing the system prompt, LeQP adaptively perturbs user queries
 446 without an additional system prompt.

447 **Evaluation on Classification Tasks.** Following (Yue et al., 2021; Chen et al., 2023a; Tong et al.,
 448 2023), we use two widely-used metrics to evaluate **privacy protection levels** by measuring model’s
 449 robustness against common attacks: (1) Local Semantic Protection Degree (P_{LS}), which exploits
 450 the *embedding inversion attack* (Qu et al., 2021) to measure the local, token-wise semantic privacy
 451 level by comparing the semantic embedding similarity between the private token and plaintext token
 452 ($P_{L,LS}$ and $P_{O,LS}$ denote the local semantic protection degree of the perturbed LLM inputs and
 453 that of the LLM outputs, respectively). (2) Global Semantic Protection Degree (P_{GS}), which adopts
 454 the *input inference attack* (Yue et al., 2021) to measure the global semantic privacy level of the
 455 perturbed LLM inputs by computing the rate of incorrect inference on partially masked tokens. Fol-
 456 lowing (Yue et al., 2021; Chen et al., 2023a), we measure the **utility level** by the accuracy (U_{ACC})
 457 of LLM responses. As shown in Table 1, the DP methods (Yue et al., 2021; Chen et al., 2023a)
 458 and the learnable perturbation method (LeQP) make the input text incoherent, significantly reduc-
 459 ing LLM comprehension and response accuracy. The anonymization method (Chen et al., 2023b)
 460 fails to fully conceal sensitive information, resulting in poor privacy-preserving performance. In
 461 contrast, PrivateChat excels across all privacy and utility metrics and achieves comparable utility
 462 to the plaintext method (i.e., plaintext user input). This superior performance is attributed to: (i)
 463 Customized encryption and the private system prompt ensure secure communications that are only
 464 interpreted by the user and the LLM. (ii) The black-box optimizer enables the generated system
 prompt to effectively guide the LLM to produce encrypted and accurate responses.

465 **Evaluation on Question-answering (Q/A) Task.** To simulate daily interactions between users
 466 and LLMs, we evaluate our method on the medical Q/A dataset. For **privacy protection level**
 467 assessment, we use the Local Semantic Protection Degree (P_{LS}) and Global Semantic Protection
 468 Degree (P_{GS}) mentioned above. Following (Xiao et al., 2023), we assess the **utility level** using three
 469 Rouge criteria: U_{Rouge_1} , U_{Rouge_2} and U_{Rouge_L} . As shown in Tab. 1, PrivateChat outperforms other
 470 methods in both privacy and utility levels. We show a Q/A chat example in Fig. 4, demonstrating
 471 that our method enables secure, effective communication between the user and the LLM.

472 **Ablation Study on System Prompt Perturbation**
 473 **Model.** Our system prompt perturbation model is de-
 474 signed to generate effective private system prompts.
 475 We first show its effectiveness by comparing our
 476 prompt with those generated by the differential privacy
 477 method (DP-based Prompt) (Chen et al., 2023a) and
 478 anonymization method (Anon-based Prompt) (Vats
 479 et al., 2023) on the SST-2 dataset (Wang et al., 2018).
 480 The DP-based Prompt incorporates random noise into
 481 the plaintext prompt, while the Anon-based Prompt re-
 482 places encryption details with synonyms. Addition-
 483 ally, we evaluate our character-level perturbation strat-
 484 egy against word-level and token-level ones. As shown in Tab. 2, our optimization-based method,
 485 enhanced by feedback from LLMs, outperforms both DP-based and Anon-based methods. Com-
 pared to word-level and token-level perturbations, character-level perturbation offers higher robust-
 ness, achieving better performance. Moreover, we assess the impact of the perturbation threshold ϵ

Table 3: Comparison of different black-box optimizers.

Models	P_{GS}	$P_{L,LS}$	$P_{O,LS}$	U_{ACC}	Training time	No. of API Calls
Random Search	0.815	0.667	0.854	0.498	4837s	1100
DDPG	0.803	0.750	0.945	0.770	5452s	1039
BAR	0.812	0.714	0.895	0.668	4176s	970
BlackVIP	0.813	0.857	0.931	0.783	1897s	440
SPSA	0.808	0.833	0.870	0.739	2383s	590
SE-SPSA	0.825	0.857	0.999	0.864	345s	80

Table 4: Results on various cloud LLMs.

Models	P_{GS}	$P_{L,LS}$	GPT-4V		Sonnet		Opus	
			$P_{O,LS}$	U_{ACC}	$P_{O,LS}$	U_{ACC}	$P_{O,LS}$	U_{ACC}
SanText	0.657	0.836	0.258	0.742	0.613	0.387	0.380	0.620
CusText+	0.571	0.433	0.231	0.769	0.377	0.623	0.446	0.554
HaS	0.536	0.479	0.127	0.873	0.277	0.723	0.183	0.817
PrivateChat	0.825	0.857	0.990	0.891	0.990	0.730	0.920	0.836

in our system prompt perturbation model. Fig. 3 shows PrivateChat’s performance under varying ε settings, where $\varepsilon = 0$ means all characters are perturbed. The privacy metric is the average of P_{GS} and P_{LS} . It is clear that as ε increases, utility improves but privacy decreases, and setting $\varepsilon = 0.7$ offers optimal overall performance.

Comparison of Optimization Methods. Our SE-SPSA is designed for effective and economical black-box optimization. To assess its effectiveness, we compare it with the original SPSA (Spall, 1992a). As shown in Fig. 5, benefiting from our baseline-based variance reduction strategy, SE-SPSA achieves more stable and accelerated convergence than the original SPSA. Furthermore, we compare our method with other black-box optimizers, such as random search (Bergstra & Bengio, 2012), DDPG (Lillicrap et al., 2015), BAR (Tsai et al., 2020) and BlackVIP (Oh et al., 2023) on the SST-2 dataset (Wang et al., 2018). As shown in Tab. 3, leveraging our variance reduction strategy, SE-SPSA significantly cuts training time and costs while achieving the best performance.

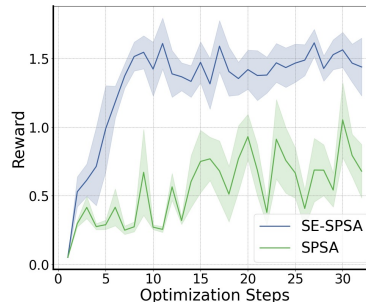


Figure 5: Comparison of reward curves among SPSA and SE-SPSA.

Experiments on Various Cloud LLMs. To demonstrate the generality of our framework, we assess its performance using popular cloud LLMs other than GPT-4 (OpenAI, 2023b), including GPT-4V (OpenAI, 2023b), Claude3 Sonnet (Anthropic, 2023), and Claude3 Opus (Anthropic, 2023) on the SST-2 dataset (Wang et al., 2018). As shown in Tab. 4, our PrivateChat exhibits impressive classification accuracy across various cloud LLMs.

5 DISCUSSION

Here, we note that compared with other privacy-preserving methods, our PrivateChat has significant differences and benefits as follows: **1) Black-box Adaptability:** Traditional privacy-preserving methods, such as homomorphic encryption and federated learning, are generally limited to service providers and inaccessible to clients without access to model parameters. In contrast, our approach does not rely on access to model parameters or architectures, making it more adaptable for real-world black-box scenarios. **2) Utility-Privacy Trade-off:** Although local differential privacy (LDP) can sanitize user queries locally, it often leads to unacceptable utility loss when a high degree of privacy is necessary. Our method addresses this trade-off between privacy protection and utility with a novel encryption framework. **3) Innovation and Inspiration:** Our work serves as an exploratory and foundational contribution to the field of LLM privacy protection. We are the first to propose an encryption framework designed for secure communication with black-box LLMs, with the potential to significantly influence future research and applications in this area.

6 CONCLUSION

In this paper, we have proposed PrivateChat, a novel private communication framework for encrypted interactions between users and cloud black-box LLMs. Our PrivateChat consists of three main modules: a client-end encryption module that encrypts user queries with the user-customized method and key, a system prompt perturbation module that safely instructs the LLM to process encrypted user queries and produce encrypted responses, and a client-end decryption module that converts the encrypted LLM responses back into plaintext. To optimize our framework, we have designed SE-SPSA, an enhanced black-box optimizer that significantly reduces the training time and costs, and improves the performance of the original SPSA via our baseline-based variance reduction strategy.

REFERENCES

- Meta AI. Introducing llama: A foundational, 65-billion-parameter language model. <https://ai.meta.com/blog/large-language-model-llama-meta-ai/>, 2023.
- Anthropic. Model card and evaluations for claude models. <https://www-files.anthropic.com/production/images/Model-Card-Claude-2.pdf>, 2023.

- 540 Yakoub Bazi, Mohamad Mahmoud Al Rahhal, Laila Bashmal, and Mansour Zuair. Vision–language
541 model for visual question answering in medical imagery. *Bioengineering*, 10(3):380, 2023.
- 542
- 543 James Bergstra and Yoshua Bengio. Random search for hyper-parameter optimization. *Journal of*
544 *machine learning research*, 13(2), 2012.
- 545 Arne Bewersdorff, Christian Hartmann, Marie Hornberger, Kathrin Seßler, Maria Bannert, Enkele-
546 jda Kasneci, Gjergji Kasneci, Xiaoming Zhai, and Claudia Nerdel. Taking the next step with
547 generative artificial intelligence: The transformative role of multimodal large language models in
548 science education. *arXiv preprint arXiv:2401.00832*, 2024.
- 549 Sai Chen, Fengran Mo, Yanhao Wang, Cen Chen, Jian-Yun Nie, Chengyu Wang, and Jamie Cui. A
550 customized text sanitization mechanism with differential privacy. In *Findings of the Association*
551 *for Computational Linguistics: ACL 2023*, pp. 5747–5758, 2023a.
- 552
- 553 Yu Chen, Tingxin Li, Huiming Liu, and Yang Yu. Hide and seek (has): A lightweight framework
554 for prompt privacy protection. *arXiv preprint arXiv:2309.03057*, 2023b.
- 555 Badhan Chandra Das, M Hadi Amini, and Yanzhao Wu. Security and privacy challenges of large
556 language models: A survey. *arXiv preprint arXiv:2402.00888*, 2024.
- 557
- 558 Jacob Devlin, Ming-Wei Chang, Kenton Lee, and Kristina Toutanova. Bert: Pre-training of deep
559 bidirectional transformers for language understanding. *arXiv preprint arXiv:1810.04805*, 2018.
- 560 Yinpeng Dong, Huanran Chen, Jiawei Chen, Zhengwei Fang, Xiao Yang, Yichi Zhang, Yu Tian,
561 Hang Su, and Jun Zhu. How robust is google’s bard to adversarial image attacks? *arXiv preprint*
562 *arXiv:2309.11751*, 2023.
- 563
- 564 Hiva Ghanbari and Katya Scheinberg. Black-box optimization in machine learning with trust region
565 based derivative free algorithm. *arXiv preprint arXiv:1703.06925*, 2017.
- 566 Yi Gui, Zhen Li, Yao Wan, Yemin Shi, Hongyu Zhang, Yi Su, Shaoling Dong, Xing Zhou, and
567 Wenbin Jiang. Vision2ui: A real-world dataset with layout for code generation from ui designs.
568 *arXiv preprint arXiv:2404.06369*, 2024.
- 569 Tianyu Han, Lisa C Adams, Jens-Michalis Papaioannou, Paul Grundmann, Tom Oberhauser,
570 Alexander Löser, Daniel Truhn, and Keno K Bressen. Medalpaca—an open-source collection
571 of medical conversational ai models and training data. *arXiv preprint arXiv:2304.08247*, 2023.
- 572
- 573 Mouhib Ibtihal, Naanani Hassan, et al. Homomorphic encryption as a service for outsourced im-
574 ages in mobile cloud computing environment. In *Cryptography: breakthroughs in research and*
575 *practice*, pp. 316–330. IGI Global, 2020.
- 576 Costel Marian Ionaşcu. Considerations about using large language models in economics: Opportu-
577 nities and implications. *Revista tinerilor economişti*, (41):149–157, 2023.
- 578
- 579 Ridhi Jain, Nicole Gervasoni, Mthandazo Ndhlovu, and Sanjay Rawat. A code centric evaluation
580 of c/c++ vulnerability datasets for deep learning based vulnerability detection techniques. In
581 *Proceedings of the 16th Innovations in Software Engineering Conference*, pp. 1–10, 2023.
- 582 Zhigang Kan, Linbo Qiao, Hao Yu, Liwen Peng, Yifu Gao, and Dongsheng Li. Protecting user
583 privacy in remote conversational systems: A privacy-preserving framework based on text saniti-
584 zation. *arXiv preprint arXiv:2306.08223*, 2023.
- 585 Christine Lai, Nicholas Jacobs, Shamina Hossain-McKenzie, Cedric Carter, Patricia Cordeiro,
586 Ifeoma Onunkwo, and Jay Johnson. Cyber security primer for der vendors, aggregators, and
587 grid operators. *Tech. Rep.*, 12, 2017.
- 588
- 589 Unggi Lee, Minji Jeon, Yunseo Lee, Gyuri Byun, Yoorim Son, Jaeyoon Shin, Hongkyu Ko, and
590 Hyeoncheol Kim. Llava-docent: Instruction tuning with multimodal large language model to
591 support art appreciation education. *arXiv preprint arXiv:2402.06264*, 2024.
- 592
- 593 Chunyuan Li, Cliff Wong, Sheng Zhang, Naoto Usuyama, Haotian Liu, Jianwei Yang, Tristan Nau-
mann, Hoifung Poon, and Jianfeng Gao. Llava-med: Training a large language-and-vision assis-
tant for biomedicine in one day. *Advances in Neural Information Processing Systems*, 36, 2024.

- 594 Timothy P Lillicrap, Jonathan J Hunt, Alexander Pritzel, Nicolas Heess, Tom Erez, Yuval Tassa,
595 David Silver, and Daan Wierstra. Continuous control with deep reinforcement learning. *arXiv*
596 *preprint arXiv:1509.02971*, 2015.
- 597 Chin-Yew Lin. Rouge: A package for automatic evaluation of summaries. In *Text summarization*
598 *branches out*, pp. 74–81, 2004.
- 600 Fenglin Liu, Xian Wu, Shen Ge, Wei Fan, and Yuexian Zou. Federated learning for vision-and-
601 language grounding problems. In *Proceedings of the AAAI conference on artificial intelligence*,
602 volume 34, pp. 11572–11579, 2020.
- 603 Fenglin Liu, Tingting Zhu, Xian Wu, Bang Yang, Chenyu You, Chenyang Wang, Lei Lu, Zhangdai-
604 hong Liu, Yefeng Zheng, Xu Sun, et al. A medical multimodal large language model for future
605 pandemics. *NPJ Digital Medicine*, 6(1):226, 2023a.
- 607 Jun Liu, Jiantao Zhou, Jinyu Tian, and Weiwei Sun. Recoverable privacy-preserving image classi-
608 fication through noise-like adversarial examples. *arXiv preprint arXiv:2310.12707*, 2023b.
- 609 Nils Lukas, Ahmed Salem, Robert Sim, Shruti Tople, Lukas Wutschitz, and Santiago Zanella-
610 Béguelin. Analyzing leakage of personally identifiable information in language models. *arXiv*
611 *preprint arXiv:2302.00539*, 2023.
- 612 Yao Mu, Junting Chen, Qinglong Zhang, Shoufa Chen, Qiaojun Yu, Chongjian Ge, Runjian Chen,
613 Zhixuan Liang, Mengkang Hu, Chaofan Tao, et al. Robocodex: Multimodal code generation for
614 robotic behavior synthesis. *arXiv preprint arXiv:2402.16117*, 2024.
- 616 Dilxat Muhtar, Zhenshi Li, Feng Gu, Xueliang Zhang, and Pengfeng Xiao. Lhrs-bot: Empow-
617 ering remote sensing with vgi-enhanced large multimodal language model. *arXiv preprint*
618 *arXiv:2402.02544*, 2024.
- 619 Seth Neel and Peter Chang. Privacy issues in large language models: A survey. *arXiv preprint*
620 *arXiv:2312.06717*, 2023.
- 621 Changdae Oh, Hyeji Hwang, Hee-young Lee, YongTaek Lim, Geunyoung Jung, Jiyoung Jung,
622 Hosik Choi, and Kyungwoo Song. Blackvip: Black-box visual prompting for robust transfer
623 learning. In *Proceedings of the IEEE/CVF Conference on Computer Vision and Pattern Recogni-*
624 *tion*, pp. 24224–24235, 2023.
- 626 OpenAI. Chatgpt. <https://openai.com/chatgpt>, 2023a.
- 627 OpenAI. Gpt-4 technical report. <https://cdn.openai.com/papers/gpt-4.pdf>, 2023b.
- 628 Zhan Qin, Jingbo Yan, Kui Ren, Chang Wen Chen, and Cong Wang. Towards efficient privacy-
629 preserving image feature extraction in cloud computing. In *Proceedings of the 22nd ACM inter-*
630 *national conference on Multimedia*, pp. 497–506, 2014.
- 632 Chen Qu, Weize Kong, Liu Yang, Mingyang Zhang, Michael Bendersky, and Marc Najork. Natural
633 language understanding with privacy-preserving bert. In *Proceedings of the 30th ACM Interna-*
634 *tional Conference on Information & Knowledge Management*, pp. 1488–1497, 2021.
- 636 Nils Reimers and Iryna Gurevych. Sentence-bert: Sentence embeddings using siamese bert-
637 networks. *arXiv preprint arXiv:1908.10084*, 2019.
- 638 James C Spall. Multivariate stochastic approximation using a simultaneous perturbation gradient
639 approximation. *IEEE transactions on automatic control*, 37(3):332–341, 1992a.
- 640 James C Spall. Accelerated second-order stochastic optimization using only function measurements.
641 In *Proceedings of the 36th IEEE Conference on Decision and Control*, volume 2, pp. 1417–1424.
642 IEEE, 1997a.
- 644 James C Spall. A one-measurement form of simultaneous perturbation stochastic approximation.
645 *Automatica*, 33(1):109–112, 1997b.
- 646 James C Spall. Adaptive stochastic approximation by the simultaneous perturbation method. *IEEE*
647 *transactions on automatic control*, 45(10):1839–1853, 2000.

- 648 James C Spall. *Introduction to stochastic search and optimization: estimation, simulation, and*
649 *control*. John Wiley & Sons, 2005.
- 650
- 651 J.C. Spall. Multivariate stochastic approximation using a simultaneous perturbation gradient ap-
652 proximation. *IEEE Transactions on Automatic Control*, 37(3):332–341, 1992b.
- 653 Robin Staab, Mark Vero, Mislav Balunović, and Martin Vechev. Beyond memorization: Violating
654 privacy via inference with large language models. *arXiv preprint arXiv:2310.07298*, 2023.
- 655
- 656 Arun James Thirunavukarasu, Darren Shu Jeng Ting, Kabilan Elangovan, Laura Gutierrez,
657 Ting Fang Tan, and Daniel Shu Wei Ting. Large language models in medicine. *Nature medicine*,
658 29(8):1930–1940, 2023.
- 659 Meng Tong, Kejiang Chen, Yuang Qi, Jie Zhang, Weiming Zhang, and Nenghai Yu. Priv-
660 infer: Privacy-preserving inference for black-box large language model. *arXiv preprint*
661 *arXiv:2310.12214*, 2023.
- 662
- 663 Yun-Yun Tsai, Pin-Yu Chen, and Tsung-Yi Ho. Transfer learning without knowing: Reprogramming
664 black-box machine learning models with scarce data and limited resources. In *International*
665 *Conference on Machine Learning*, pp. 9614–9624. PMLR, 2020.
- 666 Arpita Vats, Zhe Liu, Peng Su, Debjyoti Paul, Yingyi Ma, Yutong Pang, Zeeshan Ahmed, and Ozlem
667 Kalinli. Recovering from privacy-preserving masking with large language models. *arXiv preprint*
668 *arXiv:2309.08628*, 2023.
- 669
- 670 Alex Wang, Amanpreet Singh, Julian Michael, Felix Hill, Omer Levy, and Samuel R Bowman.
671 Glue: A multi-task benchmark and analysis platform for natural language understanding. *arXiv*
672 *preprint arXiv:1804.07461*, 2018.
- 673 Yuntao Wang, Yanghe Pan, Miao Yan, Zhou Su, and Tom H Luan. A survey on chatgpt: Ai-
674 generated contents, challenges, and solutions. *IEEE Open Journal of the Computer Society*, 2023.
- 675
- 676 Cathy Wu, Aravind Rajeswaran, Yan Duan, Vikash Kumar, Alexandre M Bayen, Sham Kakade,
677 Igor Mordatch, and Pieter Abbeel. Variance reduction for policy gradient with action-dependent
678 factorized baselines. *arXiv preprint arXiv:1803.07246*, 2018.
- 679 Yijia Xiao, Yiqiao Jin, Yushi Bai, Yue Wu, Xianjun Yang, Xiao Luo, Wenchao Yu, Xujiang Zhao,
680 Yanchi Liu, Haifeng Chen, et al. Large language models can be good privacy protection learners.
681 *arXiv preprint arXiv:2310.02469*, 2023.
- 682 Yifan Yao, Jinhao Duan, Kaidi Xu, Yuanfang Cai, Zhibo Sun, and Yue Zhang. A survey on large
683 language model (llm) security and privacy: The good, the bad, and the ugly. *High-Confidence*
684 *Computing*, pp. 100211, 2024.
- 685
- 686 Youliang Yuan, Wenxiang Jiao, Wenxuan Wang, Jen-tse Huang, Pinjia He, Shuming Shi, and
687 Zhaopeng Tu. Gpt-4 is too smart to be safe: Stealthy chat with llms via cipher. *Proceedings*
688 *of the International Conference on Learning Representations*, 2024.
- 689 Xiang Yue, Minxin Du, Tianhao Wang, Yaliang Li, Huan Sun, and Sherman SM Chow. Differential
690 privacy for text analytics via natural text sanitization. *arXiv preprint arXiv:2106.01221*, 2021.
- 691
- 692 Xiaojin Zhang, Yulin Fei, Yan Kang, Wei Chen, Lixin Fan, Hai Jin, and Qiang Yang. No free lunch
693 theorem for privacy-preserving llm inference. *arXiv preprint arXiv:2405.20681*, 2024.
- 694 Haiyan Zhao, Hanjie Chen, Fan Yang, Ninghao Liu, Huiqi Deng, Hengyi Cai, Shuaiqiang Wang,
695 Dawei Yin, and Mengnan Du. Explainability for large language models: A survey. *ACM Trans-*
696 *actions on Intelligent Systems and Technology*, 15(2):1–38, 2024.
- 697
- 698 Tingting Zhao, Hirotaka Hachiya, Gang Niu, and Masashi Sugiyama. Analysis and improvement of
699 policy gradient estimation. *Advances in Neural Information Processing Systems*, 24, 2011.
- 700 Xin Zhou, Yi Lu, Ruotian Ma, Tao Gui, Qi Zhang, and Xuan-Jing Huang. Textmixer: Mixing
701 multiple inputs for privacy-preserving inference. In *Findings of the Association for Computational*
Linguistics, pp. 3749–3762, 2023.